Journal of Science: Advanced Materials and Devices 7 (2022) 100439

Contents lists available at ScienceDirect

Journal of Science: Advanced Materials and Devices

journal homepage: www.elsevier.com/locate/jsamd

Original Article

Enrichment of cancer stem-like cells by controlling oxygen, glucose and fluid shear stress in a microfluidic spheroid culture device

Maryam Barisam [a], Fazeleh Ranjbar Niavol [b], Moslem Afrasiabi Kinj [c], Mohammad Said Saidi [a, **], Hossein Ghanbarian [d], Navid Kashaninejad [e, *]

[a] Department of Mechanical Engineering, Sharif University of Technology, Tehran, Iran
[b] Department of Stem Cells and Developmental Biology, Cell Science Research Centre, Royan Institute for Stem Biology and Technology, ACECR, Tehran, Iran
[c] Thermo and Fluids Department, Faculty of Mechanical Engineering, University of Guilan, Rasht, Iran
[d] Department of Medical Biotechnology, School of Advanced Technologies in Medicine, Shahid Beheshti University of Medical Science, Tehran, Iran
[e] Queensland Micro-and Nanotechnology Centre (QMNC), Griffith University, Nathan Campus, QLD, 4111, Australia

ARTICLE INFO

Article history:
Received 7 September 2021
Received in revised form
9 February 2022
Accepted 16 February 2022
Available online 21 February 2022

Keywords:
CSC enrichment
Microfluidic cell culture
Spheroid
U-shaped barrier

ABSTRACT

Current chemotherapies can often kill fast-growing cancer cells but are ineffective in destroying cancer stem cells (CSCs). This study aimed to investigate the effect of *in vitro* cell culture conditions on the features of lung adenocarcinoma cells (represented by A549, non-small cell type (NSCLC), cell lines) and the induction of cancer stem-like cells. For this purpose, a microfluidic system containing U-shaped arrays was designed and numerically optimized. This system was used for the three-dimensional culture of cells under a continuous laminar flow of culture medium. Numerical simulations were also performed to estimate the quiescent and necrotic zones inside the spheroids and the fluid shear stress on the cultured spheroids. Moreover, the effects of culture medium flow rate, oxygen and glucose concentrations and anoikis phenomenon on the number of $CD90^{+}$ cells and expression of stemness, epithelial-mesenchymal transition (EMT) and ATP-binding cassette (ABC)-transporters genes were investigated. The results showed that all these parameters substantially affected the enrichment of A549 cancer stem-like cells. We also investigated the effect of the CSC enrichment method, i.e., shear stress and oxygen and glucose concentrations, on resistance to cisplatin treatment. Increasing shear stress and glucose concentration and decreasing oxygen concentration led to a sharp increase in chemoresistance of cells. Interestingly, changing oxygen concentration was more significant than changing the other factors. The results of this paper can be helpful for the effective enrichment of CSCs by adjusting *in vitro* culture conditions.

1. Introduction

Cancer is one of the leading causes of death (about 10 million deaths in 2020), and lung cancer is the most common cause of cancer death (1.8 million deaths) in the world [1]. About 85% of lung cancer cases are non-small cell lung cancer (NSCLC) type. Lung adenocarcinoma and lung squamous cell carcinoma are the most common subtypes in this category [2]. The current NSCLC standard treatment is surgical resection with and without adjuvant chemotherapy for patients in the early stages of the disease. For patients with non-resectable tumors, radiotherapy is usually given in combination with chemotherapy. Despite advances in treatment, improvement in overall survival is low, and in many cases, patients experience local or distant recurrence of the disease [3]. Survival of cancer stem cells (CSCs) with drug resistance characteristics is known as the reason for the failure of current treatments and recurrence of malignant tumors [4]. The examination of drugs that specifically target CSCs is challenging due to their small population in tumor masses and CSC's instability in cell culture [5]. As such, one possible solution to tackle this bottleneck problem is to increase the population of cancer stem-like cells in a cancerous sample (CSCs enrichment) and focus on this population rich in CSCs, in order to understand the pharmacological resistance of these rare cells and identify the

* Corresponding author.
** Corresponding author.
E-mail addresses: mssaidi@sharif.edu (M.S. Saidi), n.kashaninejad@griffith.edu.au (N. Kashaninejad).
Peer review under responsibility of Vietnam National University, Hanoi.

https://doi.org/10.1016/j.jsamd.2022.100439

changes that lead to the acquisition of self-renewal and therapeutic resistance [6]. In this regards, some researchers have tried to increase CSCs by producing multicellular tumor spheroids through various protocols [7–10]. In spite of normal cells that would die due to anoikis or apoptosis induced by non-adhesion to the substrate or extracellular matrix (ECM), cancer cells could survive and acquire invasive and migratory traits [11]. Therefore, anoikis could induce a population rich in CSCs. In addition to anoikis, by applying fluid flow during the culture of spheroids and even single cells, researchers recently found that shear stress could also induce the enrichment of CSCs in the cancer cell population [12,13]. Although shear stress analysis was performed in a small range, it showed that flow hydrodynamics should always be considered as one of the factors influencing the enrichment of CSCs.

Another parameter that affects the induction of CSC enrichment is hypoxia. Hypoxia maintains the stemness of CSCs through various ways, such as induction of epithelial-mesenchymal transmission (EMT), suppression of differentiation-related genes, activation of stemness-related genes and signaling pathways, communication between endothelial cells and CSCs, and activation of reactive oxygen species [14]. It has been experimentally confirmed that the stem-like phenotype in the cancer cell population is enhanced by hypoxia [15,16].

Researchers have also found that the rate of glycolysis increases in the subpopulation of cancer stem-like cells. The switch from oxidative to glycolytic metabolism enables cancer cells to survive, proliferate, and migrate in environmental conditions with insufficient oxygen [17]. Thus, glucose concentration is another parameter that influences the induction of CSC enrichment, and some researchers have used this parameter to increase the subpopulation of CSCs in a sample or to maintain them and prevent their differentiation [18,19].

In the context of stem cell research, microfluidic platforms offer significant advantages for stem cell culture and differentiation, high-throughput screening and stem cell isolation [20]. Recently, tumor-on-a-chip platforms have been emerged that can more realistically recapitulate the key features of a tumor microenvironments. Cutting-edge advances for incorporating CSCs in microfluidic tumor-on-a-chip platforms have been comprehensively reviewed in a recent review article [21].

In the present study, for the first time to the best of our knowledge, the effects of all the four parameters of anoikis, shear stress, hypoxia, and glucose metabolism on the enrichment of CSCs are investigated. For this purpose, a microfluidic system containing U-shaped arrays with the ability to produce multicellular tumor spheroids is designed and optimized using numerical simulations. We have studied and compared the effect of culture medium (which flows through the microchannel) volumetric flow rate, glucose, and oxygen concentration in a wide range of values on an expression of the specific surface marker of pulmonary CSCs, and also some genes related to stemness, EMT and ABC-transporter. These examinations provide information about the level of CSC enrichment under the influence of these parameters. In addition, the effect of the CSC enrichment method on the therapeutic resistance of cell masses is investigated. We also use numerical simulations in accordance with our previous works [22,23], which are validated with experimental data, to estimate the distribution of oxygen and glucose concentrations inside tumor spheroids, as well as shear stress on their surface.

2. Theory

2.1. Geometry

It has been reported that rounded-bottom wells in microfluidic devices concentrate cells and create a single-spheroid in each well [24]. This curvature can also be obtained in the form of U-shaped barriers that facilitate the manufacturing process. On the other hand, in our previous studies [22,23], we showed that the concentrations of oxygen and glucose inside the spheroids grown in U-shaped barriers are much higher than those in well-type microfluidic devices, and it is also easier to study the effect of shear stress in this kind of spheroid-culture microfluidic systems. Therefore, in this study, U-shaped structures were selected as cell traps for spheroid formation. The geometry of the problem was designed, and geometric parameters were optimized to obtain higher cell trapping efficiency and oxygen and glucose concentrations inside the spheroid and lower shear stress on its surface. The design and optimization processes are provided in the supplementary information. Fig. 1(a) shows the final geometry used in the subsequent simulations.

2.2. Governing equations and boundary conditions

As mentioned above, since this study examined the effects of oxygen and glucose concentrations and shear stress applied to multicellular spheroids to enrich CSCs, the concentrations of oxygen and glucose inside the spheroids and fluid shear stress on their surface should be known. Because it is difficult to obtain this information experimentally, numerical simulations were performed to obtain such important data.

To describe the motion of the culture medium fluid that flows through the channel and around the spheroids, we used the conservation of mass (the continuity equation, Eq. (1)) together with the conservation of momentum (the Navier–Stokes equations, Eq. (2)). In using these equations, the flow was modeled as steady-state, incompressible and laminar flow. To find oxygen and glucose concentration distributions, we used the general form of convection-diffusion-reaction equation (Eq. (3)). There are three distinct regions where this equation can be simplified: A) Culture medium flow: Because there is no reaction in this region, the convection–diffusion equation (Eq. (3) without reaction term, R) can be used to find both oxygen and glucose concentrations. B) Multicellular spheroid: The motion of the fluid is negligible in this region. As such, the reaction–diffusion equation (Eq. (3) without convection term, $\rho(\vec{V}.\vec{\nabla})\vec{V}$) is applicable to obtain the oxygen and glucose concentrations. Michaelis–Menten reaction term (Eq. (4)) was used to model oxygen and glucose consumptions of the aggregated cells. C) Channel walls: Here, we assume that microchannel walls are oxygen permeable (e.g., made from polydimethylsiloxane (PDMS)). Accordingly, to obtain the oxygen concentration in this region, the diffusion equation (Eq. (3) without convection and reaction term) was solved.

$$\nabla.\vec{V} = 0 \tag{1}$$

$$\rho\left(\vec{V}.\vec{\nabla}\right)\vec{V} = -\vec{\nabla}p + \mu\nabla^2\vec{V} \tag{2}$$

$$\vec{V}.\vec{\nabla}c = \vec{\nabla}.(D\vec{\nabla}c) - R \tag{3}$$

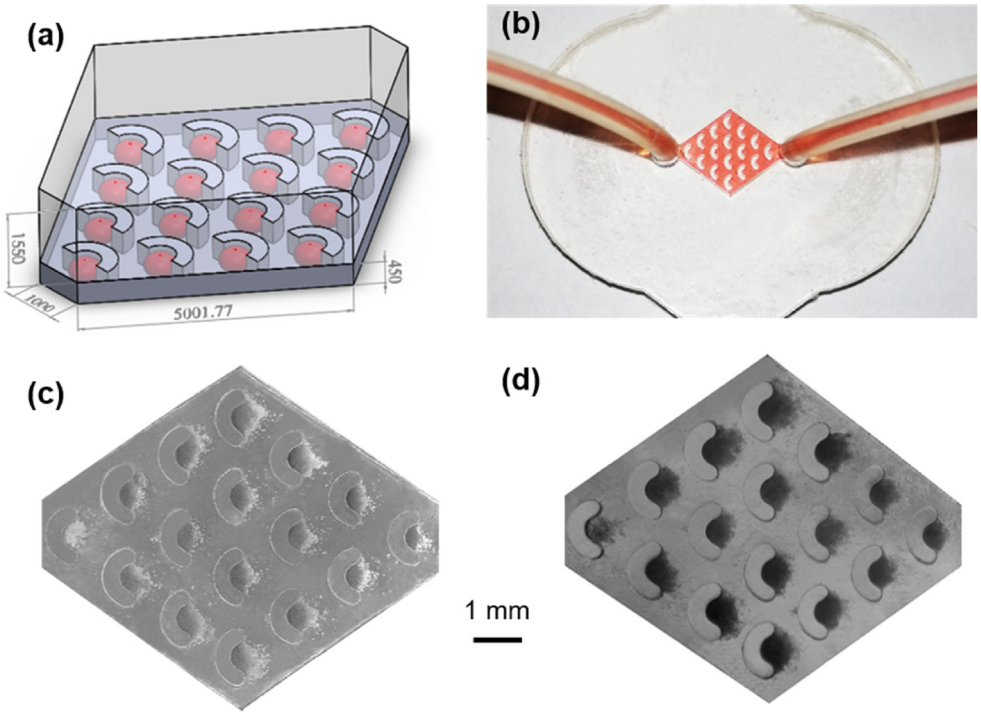

Fig. 1. (a) Geometry of the microfluidic chip used in numerical simulations for the prediction of quiescent and necrotic zones (all the dimensions are in μm), (b) a microchip used for experimental tests, and cell culture in this microchip in (c) 2 h and (d) 72 h after cell trapping in U-shaped barriers.

$$R = \frac{V_{max} c}{c + K_m} \tag{4}$$

In these equations, $\vec{V}$, ρ, p, μ, c, R, V_{max} and K_m are velocity vector, fluid density, pressure, fluid viscosity, oxygen or glucose concentration, reaction term, the maximum reaction rate and Michaelis constant, respectively. All required parameters are presented in Table S1 of the supplementary information.

A fully developed velocity profile corresponded to the flow rate (Q) and constant concentrations (c_{0,O_2} *and* $c_{0,glucose}$) were applied to the inlet. Zero pressure and no-slip boundary condition were considered for the outlet and all walls, respectively. At the upper surface of the channel wall (e.g., PDMS layer), constant concentration ($S_{PDMS\ vs\ H_2O} \times c_{0,O_2}$) was applied to model the diffusion of oxygen from the surrounding air into the culture chamber. We considered equal mass flux and concentration jump (due to differences in solubility) at the interface between every two regions (at the interface between the PDMS material and the culture medium, $c_{,PDMS} = S_{PDMS\ vs\ H_2O} \times c_{\ medium}$ and $J_{PDMS} = J_{medium}$ and at the interface between the aggregate and the culture medium, $c_{aggregate} = S_{CT\ vs\ H_2O} \times c_{\ medium}$ and $J_{CT} = J_{medium}$ were considered. J is the mass flux.). In these correlations c_{0,O_2}, $c_{0,glucose}$, $S_{PDMS\ vs\ H_2O}$, and $S_{CT\ vs\ H_2O}$ are inlet oxygen concentration, inlet glucose concentration, solubility of oxygen in PDMS vs. water and solubility of glucose or oxygen in cancerous tissue vs. water, respectively.

Depending on the availability of oxygen and nutrients, the area inside the tumor is divided into three zones: necrotic, quiescent or hypoxic, and proliferating zones. In the necrotic zone, the level of oxygen and nutrients is so low that it leads to cell death. These essential substances are readily available to the cells in the proliferating zone to facilitate their growth and proliferation. However, in the quiescent or hypoxic zone, the oxygen and nutrient levels are between these two zones, causing the cells to stay viable without proliferation. The cells located in the quiescent zone play an important role in angiogenesis and cancer progression [25]. We assumed that necrotic and quiescent regions occur at oxygen partial pressure of 2 and 10 mmHg [26] or glucose concentrations of 0.2 and 0.5 mM [27], respectively.

All the domains were meshed with an unstructured tetrahedral grid, and mesh refinement was applied to the boundaries and interfaces. We used the finite element approach to solve the governing equations in three regions. The residual values less than 10^{-6} for the continuity and the Navier–Stokes equations and 10^{-3} for all the forms of Eq. (3) were chosen as convergence criteria.

3. Experimental

3.1. Cell culture

A549 cells (purchased from Pasteur Institute of Iran) are cultured and incubated inside the cell culture flask containing high glucose Dulbecco's Modified Eagle Medium (Gibco) supplemented with 10% fetal bovine serum (FBS, Gibco) and 1% penicillin-streptomycin (Sigma–Aldrich) at 37 °C and 5% CO_2. At 70–90% confluence, the cell passages were done. For this purpose, the surface culture medium was discarded, and the cells were washed with phosphate-buffered saline (PBS, Sigma–Aldrich) without pouring directly on the cells. Next, the trypsin EDTA 0.25% was added to the cells and incubated for 3 min. The supplemented culture medium was then used to neutralize the effects of trypsin. The cells were counted with Neobar lam, and then the required amount (5×10^6 cells) was separated and centrifuged at 1500 rpm. The remaining cellular precipitate was combined with a certain amount of supplemented culture medium (1 ml) with a specific glucose concentration to be used in microfluidic device $\left(5 \times 10^6 \frac{cells}{ml}\right)$.

3.2. Fabrication of the microfluidic device

The microfluidic chip mold was micromilled in poly (methyl methacrylate) (PMMA) substrate using a computer numerical control (CNC) machine. To construct the microchips, the prepolymer and the curing agent of PDMS were mixed in the weight ratio of 10:1, and a vacuum desiccator was used to remove the air bubbles for 30 min. Then, the mixture was poured into the constructed mold, and the air bubbles were removed again in the desiccator. Finally, it was cured for 6 h at 60 °C. After peeling off from the mold and punching the input and output ports, it was bonded to another PDMS layer using oxygen plasma treatment. The completed microchip (Fig. 1(b)) was kept at 80 °C for 1 h to further strengthen the bonding.

3.3. Microchip operation

The suction mode of the syringe pump was used to establish flow into the microchip. In fact, the syringe pump draws fluid out of the microchip outlet by creating negative pressure. This method eliminates the possibility of bubble formation in case of changing the syringe and facilitate the balance of temperature and concentration of oxygen and carbon dioxide in the input culture medium by placing the container of culture medium in the incubator.

The surface coating of bovine serum albumin (BSA) may provide a potentially weak adhesion cell—substrate interaction and create a better environment for strengthening and maintaining CSCs [28]. Therefore, 0.1 g/l solution of BSA in PBS was utilized. When this solution covered the entire set, the fluid flow was cut off, and the system was incubated for 1 h.

For sterilization, the entire microfluidic system was exposed to UV light in the biosafety cabinet for 20 min, and then 70% ethyl alcohol (filtered with Corning® 0.2 μm syringe filters for further purification) was injected into the microfluidic device for 1 h. Alcohol was then removed from the system by sterile PBS flow. This protocol was used prior to every cell loading.

3.4. Cell loading and spheroid formation

According to Fig. S7, the cell trapping efficiency is around 60% for the flow rate of 3 $\mu l/min$, which was selected as the optimal value. Considering Eq. S2, it will take at least 11.3 min to have 100,000 trapped cells on the microchip for the cell density of $5 \times 10^6 cells/ml$, under the flow rate of 3 $\mu l/min$ (with a cell trapping efficiency of 60%). In the experiments, a high flow rate of cell suspension was initially considered so that the cells evenly covered the entire microstructure. The flow rate of 3 $\mu l/min$ was then applied for 15 min (the difference between experimental and theoretical cell seeding time was taken into account to consider the washing of the cells during the increase in flow rate.). During this time, the microchip was placed on an inclined plate with a 45-degree angle (this angle was obtained from the results of supplementary information based on numerical studies) to allow the cells to be trapped in U-shaped barriers. Finally, the culture medium flow was applied for 10 min to wash out the extra cells. The microchip was then transferred to the incubator, while constant continuous flow of culture medium was established for multicellular spheroid culture in the microfluidic device. The microchip was placed on the inclined plate for 2 h to allow the cells in each barrier to be compacted as a solid aggregate and then returned to a horizontal position. From cell loading to cell extraction, 72 h cultivation time was considered.

3.5. Cell extraction and off-chip spheroid analysis

We used the off-chip spheroid analysis technique to further characterize the cultured spheroids. To this aim, after 72 h of cell culture in the microfluidic system, the microchip was transferred to the sterile hood from the incubator. The culture medium inside the microchip and tubes was washed with PBS flow and collected in a sterile syringe, then the Trypsin EDTA 0.25% was used to separate the cells, and after 3 min, the culture medium with a high flow rate was once again used to collect all the cells in the syringe. Immediately, the cell solution was centrifuged for 5 min at 2000 rpm to separate the cells for flow cytometry analysis, real-time polymerase chain reaction (PCR) and drug treatment.

3.6. Hanging drop method

We used hanging drop method to better understand the effect of anoikis in CSC enrichment in spheroids cultured in both static (hanging drop) and perfusion-based (the microchip) platforms. In this method, 20 μl droplets of supplemented medium containing 6000 cells (to be closer to the spheroids produced on the microchip) were placed on the Petri dish lid containing sterile PBS. Every day, 10 μl of the culture medium of each droplet was replaced with the fresh one from the droplet side without any disturbance. After three days, the cells were used for flow cytometry or real-time PCR analysis.

3.7. Drug treatment

To evaluate drug resistance under different enrichment conditions, after three days of culture in the microfluidic system, cell aggregates were exposed to the culture medium flow rate containing 100 μM cisplatin (CISPLATIN MYLAN®, France) for 24 h. After this period, the cells were extracted, as explained in Section 3.5.

3.8. Flow cytometry

3.8.1. Quantification of CSC-like subpopulation

By isolating $CD90^+$ cells and performing functional analyzes, Yan et al. illustrated that $CD90^+$ cells have a higher tumorigenic capacity and express more stemness genes than the $CD90^-$ cells, as well as the number of created colonies and spheres, are more than those created by the $CD90^-$ subpopulation [29]. Therefore, the CD90 marker can be considered as a specific antigen for A549 CSCs. So, in this study, CD90-FITC antibody (ab11155, Abcam) and IgG1-FITC secondary antibody (ab91356, Abcam) were used to quantify the $CD90^+$ CSC-like subpopulation. After washing with PBS, the cells were stained with these antibodies and then analyzed by BD FACSCalibur ™ Flow Cytometer and FlowJo software (BD Biosciences).

3.8.2. Quantification of necrotic cells

We used propidium iodide (PI) to identify and quantify necrotic cells. PI is a red-fluorescent counterstain that is only permeable to dead cells, and its fluorescence intensity increases up to 30 folds once it is bound to the nucleus of a dead cell. As such, enumeration of PI^+ cells can be a good indication of necrotic cells present at the retrieval spheroid. Here, PI (Invitrogen, cat. no. P1304MP) with excitation and emission of 535 nm and 617 nm with similar flow cytometry protocol (laser line 488 nm) was used to quantify the subpopulation of spheroids' necrotic cells.

3.9. Real-time PCR

For total RNA extraction and cDNA synthesis, respectively, Hybrid-RTM (GeneAll) and YT4500 (Yektatajhiz) kits were used according to the manufacturers' instructions. Expression of stemness genes (OCT4 and Nanog), EMT genes (Zeb1 and Vimentin) and

ABC transporter genes (ABCB1 and ABCG2) were quantified by real-time quantitative PCR (qPCR) study using SYBR Green master mix (A325402, Ampliqon) and StepOne Real-Time PCR system (ThermoFisher). Glyceraldehyde-3-phosphate dehydrogenase (GAPDH), which is one of the most common housekeeping genes, was used as a reference gene. Forward and reverse primers for each gene are presented in Table 1.

All statistical analyses were performed using student's t-test and one way ANOVA in GraphPad Prism 8.4.0 software. The differences were significant when P-values were less than 0.05.

4. Results and discussion

For each test, the cells were loaded into the microfluidic system and trapped in the barriers, as explained in Section 3.4 (Fig. 1(c))). They grew during 72 h of cultivation, as shown in Fig. 1(d). The results suggest that the present microfluidic system is capable of producing spheroids in relatively uniform size and shape.

4.1. The effect of different parameters on CSC enrichment

This section investigates the effect of four important parameters, i.e., shear stress, oxygen and glucose concentrations, and anoikis, on the cancer stem-like cell enrichment. To systematically study the effect of each parameter, the other three parameters were kept constant.

4.1.1. Shear stress

We adjusted the amount of shear stress applied to the cellular aggregates by changing the flow rate of the culture media. Accordingly, multicellular spheroids were cultured under different flow rates and constant oxygen and glucose concentrations (c_{0,O_2} = 0.17 mM and $c_{0,glucose}$ = 4.94 mM corresponded to normal incubator oxygen concentration and low glucose DMEM) to investigate the effect of shear stress on cancer stem cell enrichment. Fig. 2 shows the results of flow cytometry and qPCR analysis for different flow rates. Numerical simulations were also performed under these conditions.

Numerical results showed that the maximum shear stress applied to the aggregates varies from an approximate value of 0.4–2 mPa with the increase of flow rate from 0.6 to 3 μl/min, which is within the allowable range for A549 cells in all cases [30]. According to the simulation results, necrosis (due to the lack of oxygen) and hypoxia occur in all the considered flow rates, and the volume of these zones decreases by increasing the flow rate (Fig. 2(d)). At Q = 0.6 μl/min, the lowest number of PI^- cells and the highest upregulation of EMT genes, i.e., Zeb1 and Vimentin, were observed, which is reasonable due to the presence of a large quiescent region (here it is equivalent to the hypoxic zone) that induces EMT [14]. By increasing the flow rate to 1.5 μl/min, cell survival increased, but there was still a large area of hypoxia, so the highest number of $CD90^+$ cells and the maximum expression of Nanog and ABCg2 were obtained. In the case of OCT4, Q = 0.6 μl/min still had the highest expression. OCT4 has been regarded as an important pluripotency marker in stem cells and is strongly related to the pathological aspect of cancer malignancy [31]. EMT markers have been connected to the progression of cancer and the acquisition of stemness properties. Co-expression of OCT4 and both EMT factors, such as Zeb1and Vimentin, could be closely involved in tumor progression [32]. By increasing the flow rate from 1.5 μl/min to 2.25 μl/min, the hypoxic zone of the aggregates decreased by approximately 13%, while cell survival remained high. The sharp decrease in the number of $CD90^+$ cells and the expression of almost all the genes (except Zeb1) at a flow rate of 2.25 μl/min could be attributed to this decrease in the hypoxic region, which affects the induction of CSC enrichment [14]. By further increasing the flow rate to 3 μl/min, the shear stress applied to the spheroids, and the mean glucose concentration inside the spheroids increased, and slight growth in the number of $CD90^+$ cells and almost all gene expression were observed. It can be concluded that the increase in shear stress and glucose concentration overcame the decrease in the hypoxic region and consistently enhanced $CD90^+$ cells and the expression of all considered genes. Previous studies confirm the present results that cancer stem cell enrichment increases with increasing glucose concentration and shear stress and decreasing oxygen concentration [12–19].

According to the above results, it is deduced that the change in the flow rate is associated with a change in shear stress on the multicellular aggregates and subsequently affects the concentrations of oxygen and glucose inside these aggregates. Therefore, it can reduce or increase the enrichment of cancer stem-like cells.

4.1.2. Oxygen concentration

In this study, we used the protocol proposed by Wright et al. to produce a low oxygen environment [33] to investigate the effect of oxygen concentration on cancer stem cell enrichment. In this investigation, the air trapped in the culture chamber had 10, 15 and 20% oxygen, which are equivalent to the oxygen concentration of 0.087, 0.13 and 0.17 mM in the culture medium, respectively. The same glucose concentration and flow rate ($c_{0,glucose}$ = 4.94 mM and Q = 1.5 μl/min, according to the previous section, maximum $CD90^+$ cells were observed at Q = 1.5 μl/min and normal oxygen condition) were used in all three cases. Experimental and numerical results are presented in Fig. 3.

Table 1
Forward and reverse primer sequence for the genes.

Genes groups	Gene name	Primer Sequence (5′→3′)	Product size (bp)
Housekeeping gene	GAPDH	F: CATGAGAAGTATGACAACAGCCT R: AGTCCTTCCACGATACCAAAGT	113
Stemness genes	OCT4	F: GTGGAGAGCAACTCCGATG R: TGCAGAGCTTTGATGTCCTG	121
	Nanog	F: AGCTACAAACAGGTGAAGAC R: GGTGGTAGGAAGAGTAAAGG	145
EMT genes	Zeb1	F: CTTCTCACACTCTGGGTCTTATTC R: CGTTCTTCCGCTTCTCTCTTAC	75
	Vimentin	F: TCTACGAGGAGGAGATGCGG R: GGTCAAGACGTGCCAGAGAC	213
ABC transporter genes	ABCG2	F: TTCCACGATATGGATTTACGG R: GTTTCCTGTTGCATTGAGTCC	83
	ABCB1	F: GTTCAGGTGGCTCTGGATAAG R: AGCGATGACGTCAGCATTAC	93

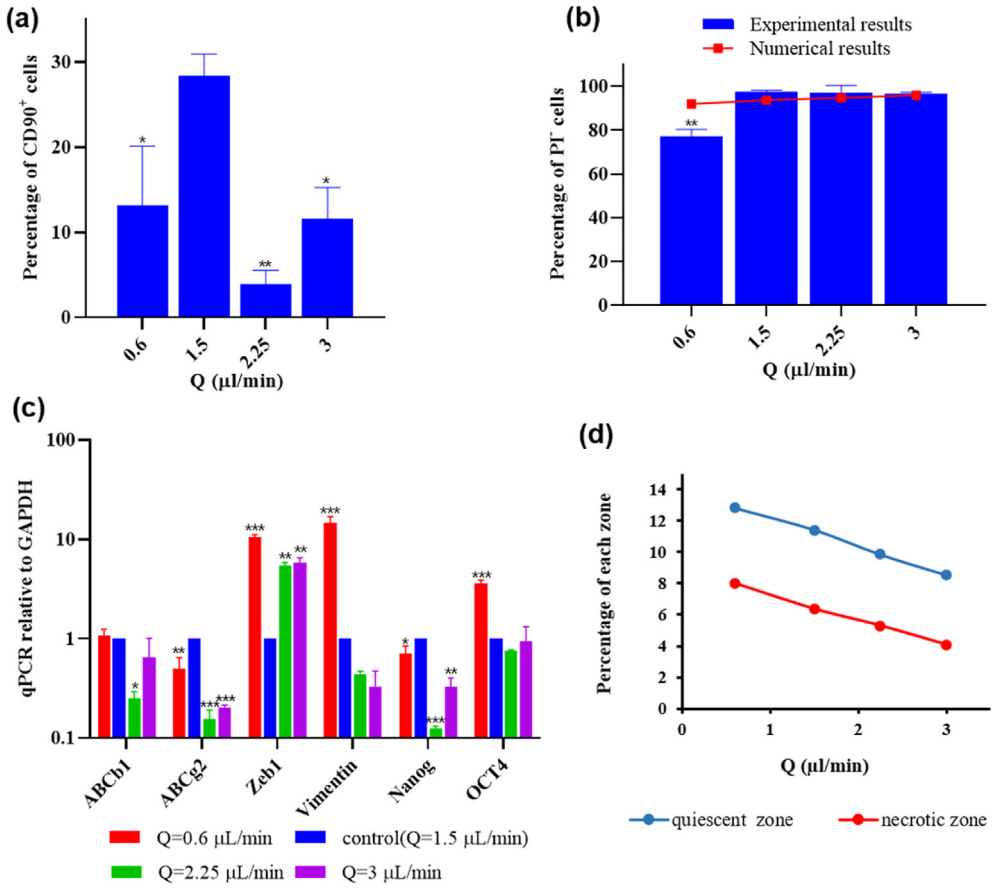

Fig. 2. The effect of flow rate on (a) percentage of $CD90^+$ cells in cell populations (experimental data), (b) percentage of PI^- cells in cell populations (experimental and numerical results), (c) gene expression (experimental data), and (d) percentage of quiescent and necrotic regions in the total volume of aggregates (numerical results). For all statistical analyses, Q = 1.5 µl/min was the control, and *, **, *** indicated that P-values were less than 0.05, 0.01, and 0.001, respectively.

According to the figure, as the oxygen concentration was decreased, the number of $CD90^+$ cells decreased sharply, and the necrotic and hypoxic (quiescent) regions grew. At an oxygen concentration of 0.087 mM, the expression of EMT genes increased sharply, which was predictable given the large hypoxic region observed in the cellular aggregates. The maximum expression of stemness genes was observed at 0.13 mM, at which the hypoxic zone is larger than the necrotic region, and the volume of this zone is larger than its equivalent volume at 0.17 mM. It has been investigated and confirmed by some researchers that hypoxia enhances the stemness of A549 cells [34,35], and the present results are consistent with the results of these papers. Also, downregulation of ABC-transporter genes was observed by decreasing the oxygen concentration from 0.17 mM.

Examination of gene expression showed that by decreasing oxygen concentration, EMT and stemness in cells were strengthened. However, a sharp decrease in the number of $CD90^+$ cells was observed. As explained by Yusuf and Fruman, the transition to a quiescent phase in cells is associated with a reduction in transcription, translation and cellular metabolism [36], so it can be argued that due to the presence of cells in the quiescent region, the rate of CD90 production in them was greatly reduced. This result was also confirmed by Fig. 2(a), because at Q = 0.6 µl/min, when the necrotic and the hypoxic regions increased, the number of $CD90^+$ cells decreased, while the EMT genes and OCT4 were upregulated. In future work, it is recommended to study the effect of oxygen concentration on longer cultivation times.

4.1.3. Glucose concentration

Metabolic activation in cancer cells has been identified as a hallmark. Warburg effect was speculated many years ago that glucose metabolism plays a driving role in tumorigenesis [37]. The signature of pluripotency metabolite in cancer cells depends on glycolysis. Glucose is essentially needed to meet the metabolic requirement of cancer cells. We studied the expression pattern of pluripotency, EMT and ABC transporters genes under various glucose concentrations in our modified system (under $c_{0,O_2} = 0.17$ mM and Q = 1.5 µl/min). First, we determined the expression levels of the genes under low glucose conditions (ranging from 1.5 to 2 mM), then subsequently, the expression rate of the genes have been analyzed under the high glucose condition (22.23 mM) in comparison with the rate of gene expression at 4.94 mM as a control.

According to Fig. 4, at a glucose concentration of 1.5 mM, the expression of Vimentin and NANOG genes raised sharply; however, Zeb 1 expression dramatically decreased. Once the glucose concentration increased, the number of $CD90^+$ cells went up sharply, and the necrotic and quiescent regions shrank. The significant overexpression of ABC transporters (ABCb1 and ABCg2) was observed at 2 mM, at which the quiescent zone was larger than the necrotic region. While the volume of these zones is smaller in 4.94 and 22.23 mM, the upregulation of ABC-transporter genes as well as Vimentin were observed by increasing the glucose concentration from 4.94 mM to 22.23 mM. The investigation of gene expression demonstrated that by decreasing glucose concentration, Vimentin and Nanog in cells were strengthened; however, a sharp decrease

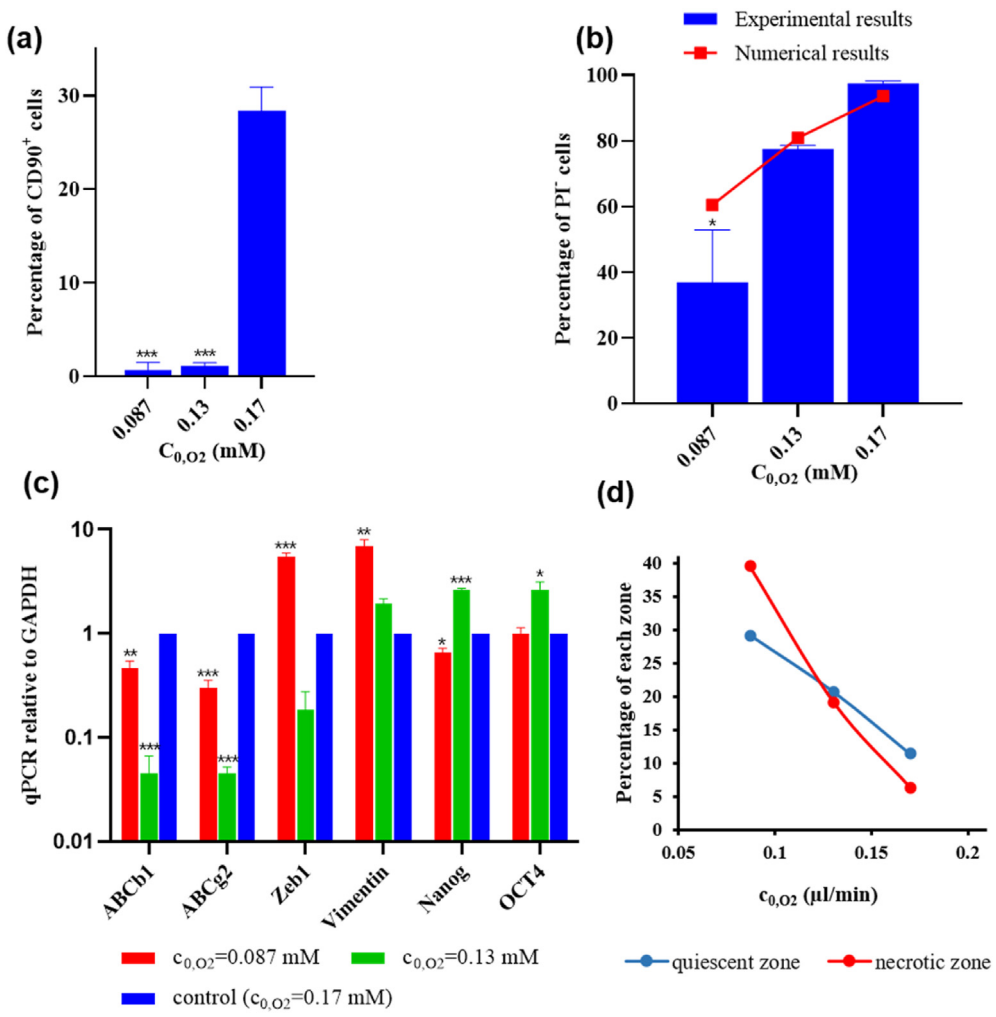

Fig. 3. The effect of culture medium oxygen concentration on (a) percentage of CD90+ cells in cell populations (experimental data), (b) percentage of PI- cells in cell populations (experimental and numerical results), (c) gene expression (experimental data), and (d) percentage of quiescent and necrotic regions in the total volume of aggregates (numerical results). For all statistical analyses, $c_{0,O_2} = 0.17$ mM was the control and *, **, *** indicated that P-values were less than 0.05, 0.01, and 0.001, respectively.

in the rate of Zeb 1 was observed. As explained by Hastreiter and Schroeder, in preserving pluripotency, Nanog is believed to be a key factor [38]. Higher expression of Nanog was associated with advanced cancer stage and shorter patient survival in lung adenocarcinoma [39].

On the other hand, changes in cell adhesion molecules play an essential part in increasing cancer cells motility and thereby promoting migration and metastasis development. In the process of EMT, epithelial cells transform and achieve mesenchymal-like properties leading to the loss of E-cadherin and the gain of Vimentin expression. Progression of tumors, metastasis and resistance to therapy is caused by EMT. During EMT process, Zeb1 seems to be a significant factor in lung cancer. However, EMT-related changes are dynamic, progressive and based on the particular factors that cause the transition, not all of which are known. Our experiments are consistent with previous results [40], indicating Zeb 1 has an indirect effect on the activation of the Vimentin signaling pathway. For more manifestation of involving factors, future studies need to be taken into consideration. With the increase in Nanog and Vimentin expression at the glucose concentration of 1.5 mM, the number of $CD90^+$ cells was expected to increase. But the large quiescent area, similar to the results of the previous sections, reduced the production rate of $CD90^+$ cells.

By enhancing glucose concentration (from 1.5 to 2 mM), ABC transporters were overexpressed compared to control (4.94 mM). The presence of glucose can activate the AMPK→Akt→ABCG2 pathway in cancer cells, responsible for promoting the CSC phenotype. In addition, ABCb1 can co-express with the ABCG2 gene identified as an indicator of self-renewal in cancer cells [41]. Interestingly, our study also revealed that a significant increase in the expression rate of Vimentin could be seen because of the expression stability caused by the highest rate of glucose stimulation (22.23 mM), which is in line with previous results [42]. Moreover, despite increasing glucose concentration, a gradual reduction of Oct 4 expression is seen. According to some previous studies [43], glucose metabolism and pluripotency can be regulated through various glucose transporters (GLUT), and future studies are needed to determine a correlation between higher glucose concentration and the reduction of Oct4 expression in our modeling.

4.1.4. Anoikis

To investigate the anoikis phenomenon, two-dimensional (2D) cell culture (in a flask) was compared with three-dimensional cell culture using the hanging drop method and the microfluidic device (microchip). The results are presented in Fig. 5. In the microchip case, all genes were upregulated compared to the 2D

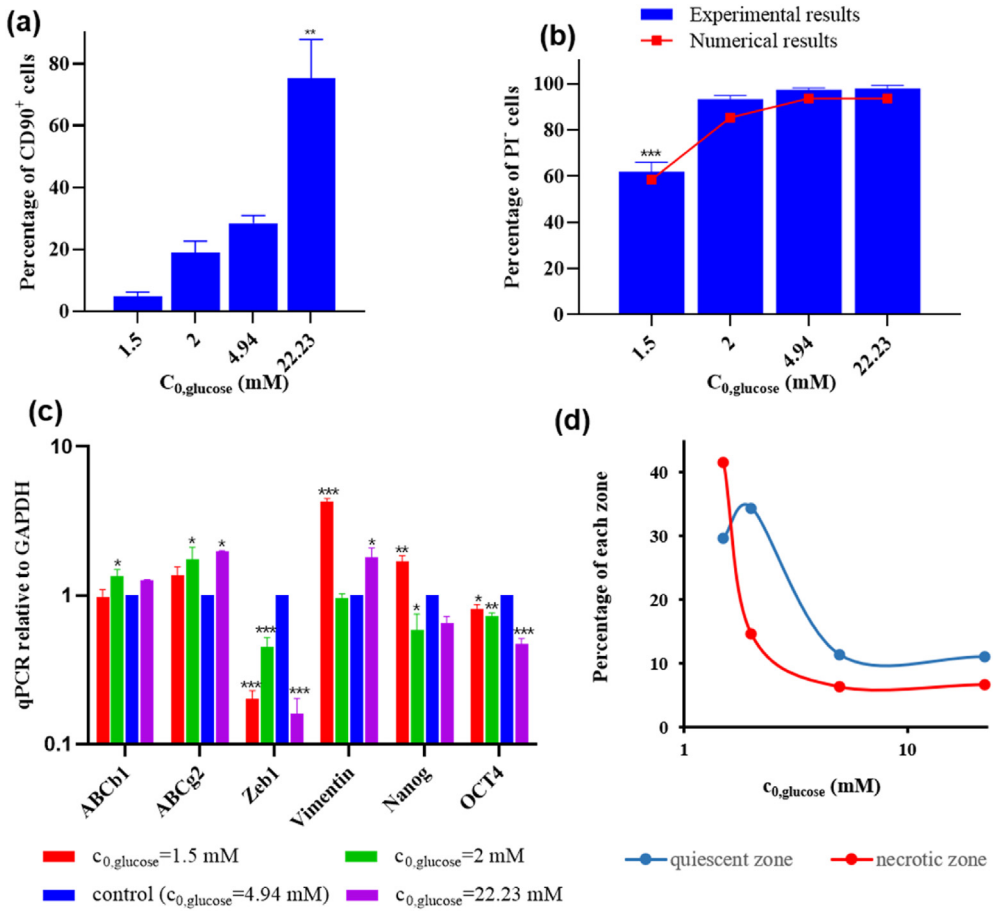

Fig. 4. The effect of culture medium glucose concentration on (a) percentage of CD90+ cells in cell populations (experimental data), (b) percentage of PI- cells in cell populations (experimental and numerical results), (c) gene expression (experimental data), and (d) percentage of quiescent and necrotic regions in the total volume of aggregates (numerical results). For all statistical analyses, $c_{0,glucose}$ = 4.94 mM was the control and *, **, *** indicated that P-values were less than 0.05, 0.01, and 0.001, respectively.

counterpart, and the percentage of $CD90^+$ cells also showed a large increase. However, for the microchip culture, in addition to anoikis, shear stress and hypoxia also acted to strengthen the cancer stem-like properties, and these increases in gene expression and $CD90^+$ cells were not the result of just anoikis. The hanging drop method was used for the specific study of anoikis. In this method, shear stress was not applied to the cells, and due to the direct oxygen supply from the surrounding air, there was no hypoxic area inside the spheroids. The mean glucose concentration in this method was much lower than the 2D culture glucose level, which led to a small area of necrosis. However, despite this decrease in the glucose concentration, all genes except Zeb1 and ABCg2, were upregulated compared to the 2D case. It means that anoikis overcame the glucose depletion and led to the increase in the expression of genes, especially stemness genes. Decreased glucose concentration affected the production of CD90 marker due to the presence of the quiescent zone as previously described, so a decrease in the percentage of $CD90^+$ cells was observed for the hanging drop method. It is concluded that anoikis enriches CSCs for A549 cell line. Previous studies [29,44,45] have shown that A549 cells cultured in the form of spheroids show more stem-like properties and a considerable increase in intercellular interactions leading to the upregulation of pluripotency and cancer stemness genes in comparison to their parental type, which confirms the present results.

4.2. Effect of CSC enrichment on chemotherapy resistance

To evaluate the effect of the CSC enrichment method on therapeutic resistance, cell aggregates were cultured in the microchip for three days under normal (c_{0,O_2} = 0.17 mM, $c_{0,glucose}$ = 4.94 mM and Q = 1.5 μl/min), high shear stress (c_{0,O_2} = 0.17 *mM*, $c_{0,glucose}$ = 4.94 *mM* and Q = 3 μl/min), high glucose (c_{0,O_2} = 0.17 mM, $c_{0,glucose}$ = 22.23 mM and Q = 1.5 μl/min) and low oxygen (c_{0,O_2} = 0.13 mM, $c_{0,glucose}$ = 4.94 mM and Q = 1.5 μl/min) conditions. After three days of culture, the culture medium containing 100 μM of cisplatin with the same oxygen and glucose concentrations as the previous three days and a flow rate of 1.5 μl/min was established in the microfluidic system. We used the same flow rate even for the case of high shear stress because all samples must be in proximity to the same amount of drug to be comparable. After 24 h of treatment, the cells were extracted from the microchip and the percentage of PI^- cells after treatment was normalized to the average percentage of PI^- cells before treatment, as shown in Fig. 6.

According to the figure, by decreasing oxygen concentration and increasing glucose concentration, chemotherapy resistance increased sharply. This was expected due to the enrichment results and was confirmed by the literature [46,47]. Although the results of the previous section confirmed a decrease in the number of $CD90^+$ cells as well as a decrease in the expression of the effective genes by increasing the flow rate from 1.5 to 3 μl/min, an increase in therapeutic

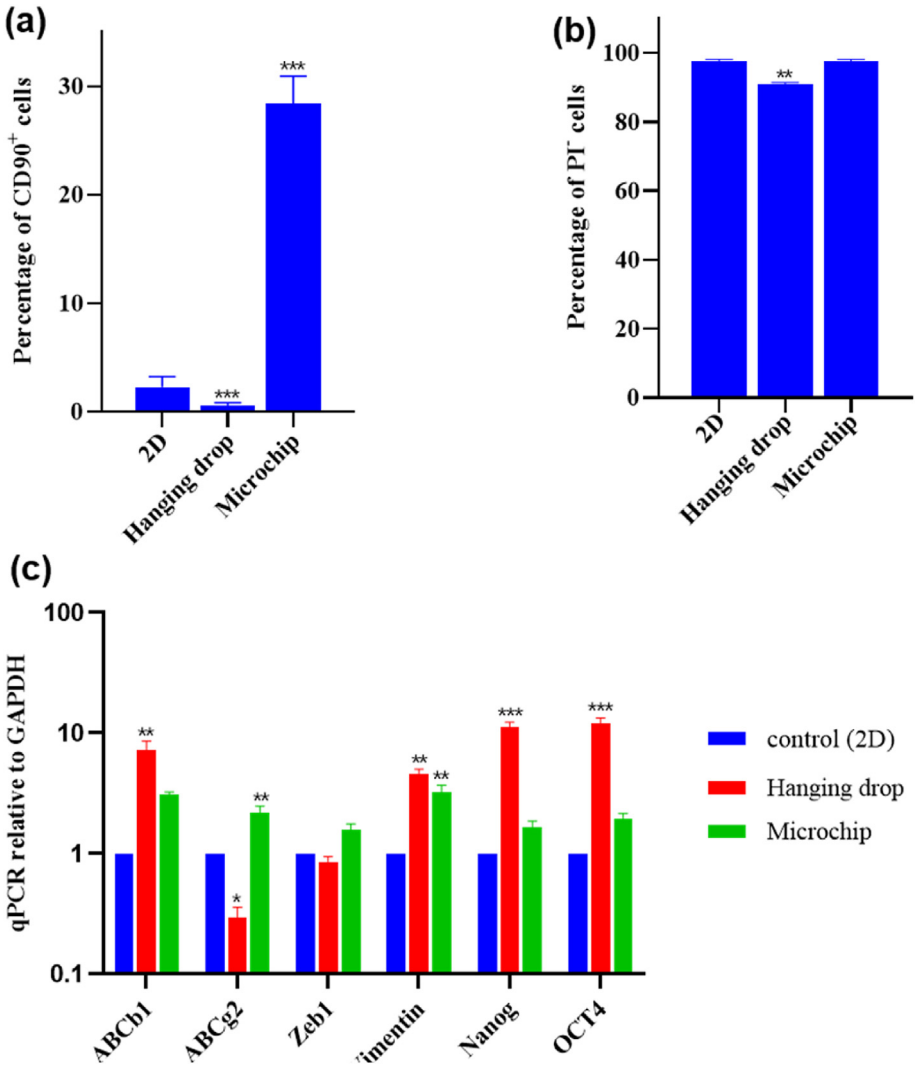

Fig. 5. The effect of anoikis on (a) percentage of CD90+ cells in cell populations, (b) percentage of PI- cells in cell populations, and (c) gene expression for three type of cell culture (2D, hanging drop and microchip) under $c_{0,O_2} = 0.17$ mM and $c_{0,glucose} = 4.94$ mM, and Q = 1.5 μl/min for just microfluidic device. For all statistical analysis, 2D was the control and *, **, *** indicated that P-values were less than 0.05, 0.01, and 0.001, respectively.

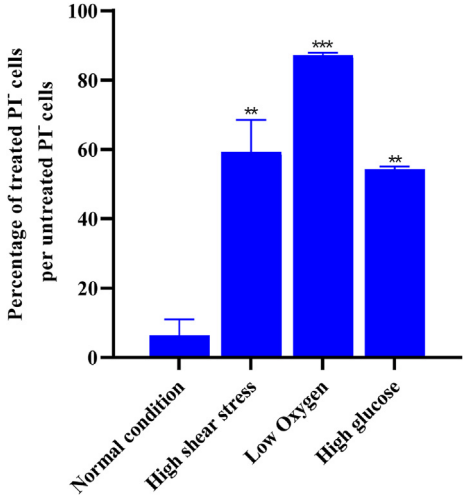

Fig. 6. The effect of CSC enrichment method, i.e., applying high shear stress, hypoxia and high glucose concentration to the cell cultured in microchip, on the therapeutic resistance after 24 h treatment with 100 μM cisplatin. For all statistical analysis, normal condition was chosen as the control and *, **, *** indicated that P-values were less than 0.05, 0.01, and 0.001, respectively.

resistance was observed. This indicated that an increase in shear stress (approximately 100%) and an average glucose concentration (approximately 6%) had a more significant effect on therapeutic resistance than a decrease in the hypoxic area (approximately 25%) and led to enhancing it. Increased therapeutic resistance due to shear stress has also been observed in the literature [12]. A 23% decrease in oxygen concentration (approximately 80% decrease in the hypoxic area), a 350% increase in glucose and a 100% increase in flow rate caused a 1260, 750 and 830% increase in cisplatin chemoresistance, respectively. This indicates that oxygen has the most significant effect on therapeutic resistance, and shear stress and glucose are in successive positions. In future studies, it is recommended to examine the effect of each parameter in a larger range to determine whether the results are valid under different conditions or not.

5. Conclusion

CSCs have a great influence on the progression, metastasis and drug resistance of cancer, so it is very important to study their enrichment inside tumor mass. On the other hand, lung cancer is one of the most common and deadly cancers worldwide. Therefore,

in this study, we tried to investigate the effect of various parameters, i.e., anoikis, shear stress, oxygen and glucose concentrations, on the induction of CSCs in lung adenocarcinoma A549 cell populations by examining the expression of stemness, EMT and ABC-transporter genes and CD90 surface marker. For this purpose, a microfluidic system including an arrangement of U-shaped arrays was designed and optimized using numerical simulations. This microchip produced cellular aggregates in relatively uniform size and shape by trapping cells in the barriers. We also used numerical simulations to estimate the oxygen and glucose concentrations and shear stress in addition to the experimental tests. The results showed that when the flow rate, the oxygen concentration, or the glucose concentration was low, large quiescent and necrotic regions were created inside the aggregates, leading to the enhancement of the expression of EMT genes. As the hypoxic region became larger than the necrotic region, the expression of stemness genes increased. The increased flow rate was associated with increased shear stress and decreased quiescent zone. Because the effect of these two parameters are opposite to each other in the induction of CSCs, it led to the appearance of a condition with minimal expression of the studied genes and the number of $CD90^{+}$ cells. Before and after this point, the presence of a large quiescent area and high shear stress enhanced CSC enrichment, respectively. As the concentrations of oxygen and glucose increased, the number of $CD90^{+}$ cells increased uniformly. This increase did not, in all cases, indicate an increase in the number of CSCs-like. Because when large quiescent areas were formed within the aggregates, despite the overexpression of stemness and EMT genes, the number of $CD90^{+}$ cells decreased, which can be assumed that it was due to the reduction in protein production in these areas. In future studies, this phenomenon can be studied exclusively. The microchip cell culture showed a higher number of $CD90^{+}$ cells and higher expression of all three gene groups than the two-dimensional culture. This increase in gene expression and surface markers was due to the phenomena of anoikis, shear stress and hypoxia. The hanging drop method was used to study the anoikis phenomenon separately. The results indicated that stemness and EMT genes expression increased compared to the two-dimensional culture, so anoikis can enrich A549 CSCs-like. In this research, the effect of each of the mentioned parameters on the cisplatin therapeutic resistance was investigated. The results illustrated that by increasing shear stress and glucose concentration and decreasing oxygen concentration, the chemoresistance increased sharply. Oxygen concentration and shear stress had a more significant effect on therapeutic resistance, respectively. This study showed how these parameters, namely anoikis, shear stress, and the concentrations of oxygen and glucose, affect cancer progression, so they can be used to regulate the appropriate conditions for the effective enrichment of CSCs.

6. Limitations and future work

The present study investigated the effect of environmental parameters on the enrichment of CSCs of a specific cell line (A549 cells). It is suggested that such investigation be performed for different cancer cell lines in future studies, and the role of each of these parameters on the development of cancer stem-like cells in their population be determined. Current work studied the expression of genes associated with CSCs under the influence of mentioned factors. However, to understand how the production of proteins related to those genes changes, it is necessary to use analytical techniques such as Western blotting in future works. This research investigated therapeutic resistance to just one type of chemotherapy drug. In future studies, it is recommended that more diverse drugs, as well as combination drugs, be considered to determine which drugs are more effective in killing CSCs enriched by these methods.

Author contributions

The main idea, formal analysis and investigation, M.B and N.K.; Methodology, M.B., M.S.S. and H.G.; Numerical simulation, M.B.; Resources, M.B. and F.R.N.; Experimental tests, M.B. and M.A.K.; Data acquisition and visualization, M.B. and M.A.K.; Writing original paper draft, M.B.; Biological discussion, M.B. and F.R.N., Review and editing, M.S.S., H.G. and N.K.; Supervision, M.S.S. and N.K.; project administration and funding acquisition, M.S.S.

Declaration of competing interest

The authors declare that they have no known competing financial interests or personal relationships that could have appeared to influence the work reported in this paper.

Acknowledgments

M.S.S. and M.B. acknowledge Iran National Science Foundation for the financial support under contract number 97012039.

Appendix A. Supplementary data

Supplementary data to this article can be found online at https://doi.org/10.1016/j.jsamd.2022.100439.

References

[1] J. Ferlay, M. Ervik, F. Lam, M. Colombet, L. Mery, M. Piñeros, A. Znaor, I. Soerjomataram, F. Bray, Global Cancer Observatory: Cancer Today 2018, International Agency for Research on Cancer, Lyon, 2020.
[2] R.S. Herbst, D. Morgensztern, C. Boshoff, The biology and management of non-small cell lung cancer, Nature 553 (2018) 446–454.
[3] J. Zhu, R. Li, E. Tiselius, R. Roudi, O. Teghararian, C. Suo, H. Song, Immunotherapy (Excluding Checkpoint Inhibitors) for Stage I to III Non-small Cell Lung Cancer Treated with Surgery or Radiotherapy with Curative Intent, Cochrane Database of Systematic Reviews, 2017.
[4] C.T. Jordan, M.L. Guzman, M. Noble, Cancer stem cells, N. Engl. J. Med. 355 (2006) 1253–1261.
[5] P.B. Gupta, T.T. Onder, G. Jiang, K. Tao, C. Kuperwasser, R.A. Weinberg, E.S. Lander, Identification of selective inhibitors of cancer stem cells by high-throughput screening, Cell 138 (2009) 645–659.
[6] H. Liu, J.D. Lathia, Cancer Stem Cells: Targeting the Roots of Cancer, Seeds of Metastasis, and Sources of Therapy Resistance, Elsevier, 2016.
[7] W. Rao, S. Zhao, J. Yu, X. Lu, D.L. Zynger, X. He, Enhanced enrichment of prostate cancer stem-like cells with miniaturized 3D culture in liquid core-hydrogel shell microcapsules, Biomaterials 35 (2014) 7762–7773.
[8] C. Morata-Tarifa, G. Jiménez, M.A. García, J.M. Entrena, C. Griñán-Lisón, M. Aguilera, M. Picon-Ruiz, J.A. Marchal, Low adherent cancer cell subpopulations are enriched in tumorigenic and metastatic epithelial-to-mesenchymal transition-induced cancer stem-like cells, Sci. Rep. 6 (2016) 1–13.
[9] X. Guo, Y. Chen, W. Ji, X. Chen, C. Li, R. Ge, Enrichment of cancer stem cells by agarose multi-well dishes and 3D spheroid culture, Cell Tissue Res. 375 (2019) 397–408.
[10] H. Pandit, Y. Li, X. Li, W. Zhang, S. Li, R.C. Martin, Enrichment of cancer stem cells via β-catenin contributing to the tumorigenesis of hepatocellular carcinoma, BMC Cancer 18 (2018) 1–10.
[11] L.A. Liotta, E. Kohn, Cancer and the homeless cell, Nature 430 (2004) 973–974.
[12] C.K. Ip, S.-S. Li, M.Y. Tang, S.K. Sy, Y. Ren, H.C. Shum, A.S. Wong, Stemness and chemoresistance in epithelial ovarian carcinoma cells under shear stress, Sci. Rep. 6 (2016) 1–11.
[13] U.L. Triantafillu, S. Park, N.L. Klaassen, A.D. Raddatz, Y. Kim, Fluid shear stress induces cancer stem cell-like phenotype in MCF7 breast cancer cell line without inducing epithelial to mesenchymal transition, Int. J. Oncol. 50 (2017) 993–1001.
[14] M. Najafi, B. Farhood, K. Mortezaee, E. Kharazinejad, J. Majidpoor, R. Ahadi, Hypoxia in solid tumors: a key promoter of cancer stem cell (CSC) resistance, J. Cancer Res. Clin. Oncol. 146 (2020) 19–31.

[15] J.M. Heddleston, Z. Li, R.E. McLendon, A.B. Hjelmeland, J.N. Rich, The hypoxic microenvironment maintains glioblastoma stem cells and promotes reprogramming towards a cancer stem cell phenotype, Cell Cycle 8 (2009) 3274–3284.
[16] J. Lan, H. Lu, D. Samanta, S. Salman, Y. Lu, G.L. Semenza, Hypoxia-inducible factor 1-dependent expression of adenosine receptor 2B promotes breast cancer stem cell enrichment, Proc. Natl. Acad. Sci. Unit. States Am. 115 (2018) E9640–E9648.
[17] E.M. De Francesco, F. Sotgia, M.P. Lisanti, Cancer stem cells (CSCs): metabolic strategies for their identification and eradication, Biochem. J. 475 (2018) 1611–1634.
[18] K. Shibuya, M. Okada, S. Suzuki, M. Seino, S. Seino, H. Takeda, C. Kitanaka, Targeting the facilitative glucose transporter GLUT1 inhibits the self-renewal and tumor-initiating capacity of cancer stem cells, Oncotarget 6 (2015) 651.
[19] S.-H. Lin, T. Liu, X. Ming, Z. Tang, L. Fu, P. Schmitt-Kopplin, B. Kanawati, X.-Y. Guan, Z. Cai, Regulatory role of hexosamine biosynthetic pathway on hepatic cancer stem cell marker CD133 under low glucose conditions, Sci. Rep. 6 (2016) 1–10.
[20] Q. Zhang, R.H. Austin, Applications of microfluidics in stem cell biology, Bionanoscience 2 (2012) 277–286, https://doi.org/10.1007/s12668-012-0051-8.
[21] N. Kashaninejad, M.R. Nikmaneshi, H. Moghadas, A. Kiyoumarsi Oskouei, M. Rismanian, M. Barisam, M.S. Saidi, B. Firoozabadi, Organ-Tumor-on-a-Chip for chemosensitivity assay: a critical review, Micromachines 7 (2016), https://doi.org/10.3390/mi7080130.
[22] M. Barisam, M.S. Saidi, N. Kashaninejad, N.-T. Nguyen, Prediction of necrotic core and hypoxic zone of multicellular spheroids in a microbioreactor with a U-shaped barrier, Micromachines 9 (2018) 94.
[23] M. Barisam, M.S. Saidi, N. Kashaninejad, R. Vadivelu, N.-T. Nguyen, Numerical simulation of the behavior of toroidal and spheroidal multicellular aggregates in microfluidic devices with microwell and U-shaped barrier, Micromachines 8 (2017) 358.
[24] K. Moshksayan, N. Kashaninejad, M.E. Warkiani, J.G. Lock, H. Moghadas, B. Firoozabadi, M.S. Saidi, N.-T. Nguyen, Spheroids-on-a-chip: recent advances and design considerations in microfluidic platforms for spheroid formation and culture, Sensor. Actuator. B Chem. 263 (2018) 151–176.
[25] J. Xu, G. Vilanova, H. Gomez, A mathematical model coupling tumor growth and angiogenesis, PLoS One 11 (2016), e0149422.
[26] M. Datta, L.E. Via, W. Chen, J.W. Baish, L. Xu, C.E. Barry, R.K. Jain, Mathematical model of oxygen transport in tuberculosis granulomas, Ann. Biomed. Eng. 44 (2016) 863–872.
[27] A.R. Jackson, C.-Y.C. Huang, M.D. Brown, W. Yong Gu, 3D Finite Element Analysis of Nutrient Distributions and Cell Viability in the Intervertebral Disc: Effects of Deformation and Degeneration, 2011.
[28] W. Zhang, D.S. Choi, Y.H. Nguyen, J. Chang, L. Qin, Studying cancer stem cell dynamics on PDMS surfaces for microfluidics device design, Sci. Rep. 3 (2013) 1–8.
[29] X. Yan, H. Luo, X. Zhou, B. Zhu, Y. Wang, X. Bian, Identification of CD90 as a marker for lung cancer stem cells in A549 and H446 cell lines, Oncol. Rep. 30 (2013) 2733–2740.
[30] S.-C. Lien, S.-F. Chang, P.-L. Lee, S.-Y. Wei, M.D.-T. Chang, J.-Y. Chang, J.-J. Chiu, Mechanical regulation of cancer cell apoptosis and autophagy: roles of bone morphogenetic protein receptor, Smad1/5, and p38 MAPK, Biochim. Biophys. Acta Mol. Cell Res. 1833 (2013) 3124–3133.
[31] Y. Teng, X. Wang, Y. Wang, D. Ma, Wnt/β-catenin signaling regulates cancer stem cells in lung cancer A549 cells, Biochem. Biophys. Res. Commun. 392 (2010) 373–379.
[32] R. Zhang, J. Xia, Y. Wang, M. Cao, D. Jin, W. Xue, Y. Huang, H. Chen, Co-expression of stem cell and epithelial mesenchymal transition markers in circulating tumor cells of bladder cancer patients, OncoTargets Ther. 13 (2020) 10739.
[33] W.E. Wright, J.W. Shay, Inexpensive low-oxygen incubators, Nat. Protoc. 1 (2006) 2088–2090.
[34] Y. Wang, M. Jiang, Z. Li, J. Wang, C. Du, L. Yanyang, Y. Yu, X. Wang, N. Zhang, M. Zhao, Hypoxia and TGF-β1 lead to endostatin resistance by cooperatively increasing cancer stem cells in A549 transplantation tumors, Cell Biosci. 5 (2015) 1–10.
[35] M. Zhao, Y. Zhang, H. Zhang, S. Wang, M. Zhang, X. Chen, H. Wang, G. Zeng, X. Chen, G. Liu, Hypoxia-induced cell stemness leads to drug resistance and poor prognosis in lung adenocarcinoma, Lung Cancer 87 (2015) 98–106.
[36] I. Yusuf, D.A. Fruman, Regulation of quiescence in lymphocytes, Trends Immunol. 24 (2003) 380–386.
[37] O. Warburg, On the origin of cancer cells, Science 123 (1956) 309–314.
[38] S. Hastreiter, T. Schroeder, Nanog dynamics in single embryonic stem cells, Cell Cycle 15 (2016) 770–771.
[39] S.-H. Chiou, M.-L. Wang, Y.-T. Chou, C.-J. Chen, C.-F. Hong, W.-J. Hsieh, H.-T. Chang, Y.-S. Chen, T.-W. Lin, H.-S. Hsu, Coexpression of Oct4 and Nanog enhances malignancy in lung adenocarcinoma by inducing cancer stem cell–like properties and epithelial–mesenchymal transdifferentiation, Cancer Res. 70 (2010) 10433–10444.
[40] R.M. Gemmill, J. Roche, V.A. Potiron, P. Nasarre, M. Mitas, C.D. Coldren, B.A. Helfrich, E. Garrett-Mayer, P.A. Bunn, H.A. Drabkin, ZEB1-responsive genes in non-small cell lung cancer, Cancer Lett. 300 (2011) 66–78.
[41] P. Liu, J. Liao, Z. Tang, W. Wu, J. Yang, Z. Zeng, Y. Hu, P. Wang, H. Ju, R. Xu, Metabolic regulation of cancer cell side population by glucose through activation of the Akt pathway, Cell Death Differ. 21 (2014) 124–135.
[42] C. Phoomak, K. Vaeteewoottacharn, A. Silsirivanit, C. Saengboonmee, W. Seubwai, K. Sawanyawisuth, C. Wongkham, S. Wongkham, High glucose levels boost the aggressiveness of highly metastatic cholangiocarcinoma cells via O-GlcNAcylation, Sci. Rep. 7 (2017) 1–12.
[43] D.R. Christensen, P.C. Calder, F.D. Houghton, GLUT3 and PKM2 regulate OCT4 expression and support the hypoxic culture of human embryonic stem cells, Sci. Rep. 5 (2015) 1–14.
[44] R. Roudi, Z. Madjd, M. Ebrahimi, A. Najafi, A. Korourian, A. Shariftabrizi, A. Samadikuchaksaraei, Evidence for embryonic stem-like signature and epithelial-mesenchymal transition features in the spheroid cells derived from lung adenocarcinoma, Tumor Biol. 37 (2016) 11843–11859.
[45] M.M. Balla, H.D. Yadav, B. Pandey, Tumorsphere assay provides a better in vitro method for cancer stem-like cells enrichment in A549 lung adenocarcinoma cells, Tissue Cell 60 (2019) 21–24.
[46] H. Doktorova, J. Hrabeta, M.A. Khalil, T. Eckschlager, Hypoxia-induced chemoresistance in cancer cells: the role of not only HIF-1, Biomed. Pap. Med. Fac. Palacky Univ. Olomouc Czech Repub. 159 (2015).
[47] I.-P. Yang, Z.-F. Miao, C.-W. Huang, H.-L. Tsai, Y.-S. Yeh, W.-C. Su, T.-K. Chang, S.-f. Chang, J.-Y. Wang, High blood sugar levels but not diabetes mellitus significantly enhance oxaliplatin chemoresistance in patients with stage III colorectal cancer receiving adjuvant FOLFOX6 chemotherapy, Therapeut. Adv. Med. Oncol. 11 (2019), 1758835919866964.